Journal of Molecular Spectroscopy 252 (2008) 230–238

Contents lists available at ScienceDirect

Journal of Molecular Spectroscopy

journal homepage: www.elsevier.com/locate/jms

The ν_7, ν_8, and ν_{11} bands of propynal, C_2HCHO, in the 650 cm^{-1} region

A.R.W. McKellar [a,*], J.K.G. Watson [a], Li-Kang Chu [b,1], Yuan-Pern Lee [b,c]

[a] Steacie Institute for Molecular Sciences, National Research Council of Canada, Ottawa, Ontario, Canada K1A 0R6
[b] Department of Applied Chemistry and Institute of Molecular Science, National Chiao Tung University, 1001 Ta-Hsueh Road, Hsinchu 30010, Taiwan, ROC
[c] Institute of Atomic and Molecular Sciences, Academia Sinica, Taipei 10617, Taiwan, ROC

ARTICLE INFO

Article history:
Received 8 August 2008
Available online 10 September 2008

Keywords:
Propynal
Infrared
Coriolis
Fermi

ABSTRACT

The infrared spectrum of propynal, C_2HCHO, is studied at high resolution (0.003 cm^{-1}) in the range 570–640 cm^{-1}. The relatively intense ν_{11} (C≡C–H out-of-plane bend, 693 cm^{-1}) and ν_7 (C≡C–H in-plane bend, 651 cm^{-1}) fundamental bands are linked by a strong *a*-type Coriolis interaction. The somewhat weaker ν_8 (CCO in-plane bend, 614 cm^{-1}) fundamental has a significant Fermi-type interaction with the "dark" background state $3\nu_9$ (~618 cm^{-1}). About 1400 lines are assigned and analyzed in terms of a four-state fit in order to obtain accurate band origins, rotational and centrifugal distortion parameters, and Fermi and Coriolis interaction parameters. This represents the first systematic high-resolution infrared study of propynal.

1. Introduction

Propynal is a simple six-atomic aldehyde that may be thought of as an acetylene molecule with a carbonyl group substituting for one hydrogen atom, or alternately as a formaldehyde molecule with a C_2H group substituting for one hydrogen atom. Although it is not commercially available, propynal can be prepared relatively easily and stored indefinitely with refrigeration. It also remains reasonably stable at room temperature as a low pressure gas. Propynal has been detected by radio astronomy in interstellar clouds [1] where its abundance and formation mechanism have been of special interest [2].

Microwave spectra of propynal were first reported in 1955 by Howe and Goldstein [3]. Subsequently, Costain and Morton [4] obtained a molecular structure based on microwave observations of fifteen isotopic species. A more detailed study of the ground vibrational state, based on microwave and millimeter wave data, was reported by Winnewisser [5]. Propynal exhibits a rich electronic spectrum in the violet to near ultraviolet region, which was studied in detail by Brand et al. [6,7]. Based on this work, and on low resolution infrared and Raman spectra [8,9], a complete assignment of all twelve vibrational modes was obtained [7]. More recently, the electronic spectrum of propynal has been utilized for a variety of studies involving quantum beat spectroscopy, intersystem crossing effects, radiationless transitions and stimulated emission pumping [10].

However, infrared studies of propynal since the original work of [8,9] have been relatively limited, and, to our knowledge, the present paper represents the first broad band high resolution infrared study of propynal. Takami and co-workers [11–13] reported a series of infrared-microwave double resonance measurements of propynal isotopes which revealed numerous perturbations in the rotational levels of excited states around 3000 cm^{-1}. Jones [14] reported somewhat similar double-resonance and two-photon data based on CO_2 laser probes in the 940 cm^{-1} region, and also gave some preliminary excited state microwave results. Ultraviolet–infrared double resonance has also been demonstrated [15]. Finally, in 1996 Tavladorakis and Parkin reported medium-resolution infrared spectra of the propynal isotope C_2HCDO in the 670 cm^{-1} [16] and 3325 cm^{-1} [17] regions.

In this paper, we analyze the spectrum of normal propynal, C_2HCHO, in the 570–740 cm^{-1} region as recorded at a resolution of about 0.003 cm^{-1} with a sample temperature and pressure of about 215 K and 0.15 Torr, respectively. This region includes the strong ν_7 (~651 cm^{-1}) and ν_{11} (~693 cm^{-1}) fundamental bands, as well as the somewhat weaker ν_8 (~614 cm^{-1}) fundamental band, and the $3\nu_9$ level (~618 cm^{-1}) which is mixed with ν_8. The extensive Coriolis- and Fermi-type interactions among these excited vibrational states (7^1, 11^1, 8^1, and 9^3), and with additional states not explicitly considered here, result in a rather challenging analysis. This challenge involved not so much the rotational assignments of transitions (though these were sometimes tricky) but rather the effort to fit all the assigned lines to something approaching the experimental precision. In the end, we believe that we have achieved a good understanding of these vibrational states and their interactions.

* Corresponding author. Fax: +1 613 991 2648.
E-mail address: robert.mckellar@nrc-cnrc.gc.ca (A.R.W. McKellar).
[1] Present address: Department of Chemistry and Biochemistry, Georgia Institute of Technology, 901 Atlantic Drive, Atlanta, GA 30332-0400, USA.

0022-2852/$ - see front matter Crown Copyright © 2008 Published by Elsevier Inc. All rights reserved.
doi:10.1016/j.jms.2008.09.002

2. Experimental details

Previous spectroscopic investigators have usually prepared propynal by means of the oxidation of propargyl alcohol with chromic oxide. We used instead a method described by McNab et al. [18] involving vacuum pyrolysis of commercially available ethyl propiolate (diprop-2-ynyl ether) at about 750 °C, following their recipe closely except that we used two liquid nitrogen traps following the quartz pyrolysis tube. At first, we were disappointed by the results since the infrared spectrum of the pyrolysis product seemed to indicate the presence of mostly propyne and acetylene (and likely also allene), with little propynal. But then we obtained good results after realizing that the real propynal was the least volatile portion of our product, a pale yellow liquid which remained when the sample was warmed to room temperature.

The spectra were recorded using the full resolution of a modified [19] Bomem DA8 Fourier transform spectrometer (maximum optical path difference = 4.5 m, nominal unapodized resolution ≈0.0022 cm^{-1}, measured line widths ≈0.0027 cm^{-1}). The 2 m absorption cell [20,21] was set for a path length of 8 m, and cooled to a temperature of about 215 K in order to reduce the strength of hot bands in the spectrum. Two spectra were obtained, with sample pressures of about 0.14 and 0.22 Torr, covering the range 570–740 cm^{-1}. This resulted in very strong absorption in the central region around 660–680 cm^{-1}, and in retrospect we should also have recorded a spectrum with significantly lower pressure in order to clarify the central region (though it is so congested that higher resolution would also be required). As well, it later became evident that we should have recorded a wider spectral range, since weak, but easily assigned, propynal transitions continue below 570 and above 740 cm^{-1}, even at 215 K.

3. Results and analysis

3.1. The propynal molecule

Propynal is a planar near-prolate ($A > B \approx C$) asymmetric rotor belonging to the C_s point group, with a notably large A rotational constant of 2.27 cm^{-1}. Its vibrational states [7] in the energy range below 800 cm^{-1} are shown in Fig. 1. The ground state and in-plane vibrations have A' symmetry, while out-of-plane fundamental vibrations and their odd multiples have A'' symmetry. In Fig. 1, the A' vibrational states are labeled in normal type and the A'' states are labeled in italics. Vibration-rotation bands linking two states of A' symmetry, or two states of A'' symmetry, exhibit a- and/or b-type selection rules, whereas those bands linking states of unlike symmetry exhibit c-type selection rules. The rotational structure of the ν_{11} fundamental is thus c-type, while the ν_7 and ν_8 fundamentals are a, b-hybrid bands.

For visualization and spectral simulations we made use of the JB95 [22] and PGopher [23] programs. The line position analyses were carried out in terms of the A-reduced asymmetric rotor Hamiltonian [24] using our own asymmetric rotor fitting programs [25,26], with unresolved asymmetry doublets fitted to the mean of their calculated positions. Perturbations among different vibrational states are very important for propynal. Interactions between two states of the same symmetry include a homogeneous Fermi-type term, a c-type Coriolis term, and various higher-order terms. Interactions between states of different symmetry (A' and A'') include a- and b-type Coriolis terms plus higher-order terms. The matrix elements used here for the interaction between vibrational states X and Y of the same symmetry, or states X and Z of different symmetry, were as follows:

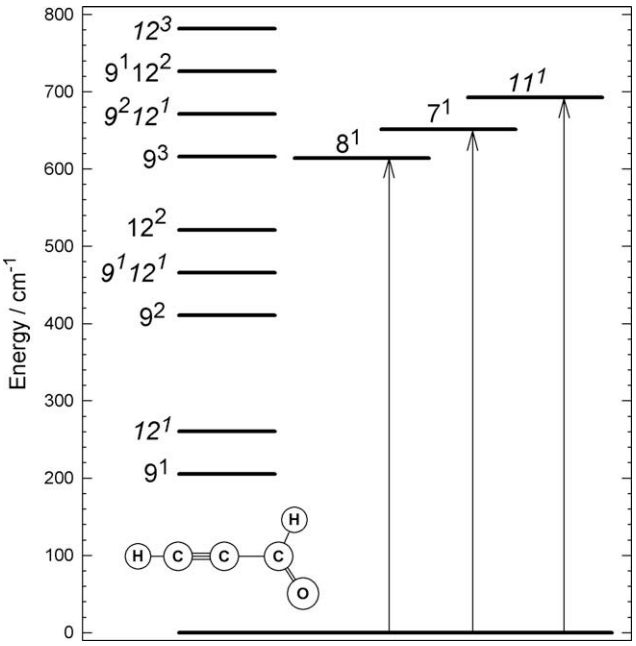

Fig. 1. Vibrational levels of the propynal molecule below 800 cm^{-1}. States of A' symmetry are labeled in normal script and those of A'' symmetry in italics. The arrows indicate the fundamental infrared absorption bands studied in the present paper.

$$\langle X,k \mid H \mid Y,k\rangle = W(X,Y) + Z_2(X,Y)k^2$$
$$\langle X,k \mid H \mid Y,k\pm 1\rangle = (1/2)[\pm G_c(X,Y) + Z_3(X,Y)(2k\pm 1)] \times [J(J+1) - k(k\pm 1)]^{1/2}$$
$$\langle X,k \mid H \mid Y,k\pm 2\rangle = (1/2)Z_1(X,Y)\{[J(J+1) - k(k\pm 1)] \times [J(J+1) - (k\pm 1)(k\pm 2)]\}^{1/2}$$
$$\langle X,k \mid H \mid Z,k\rangle = [G_a(X,Z) + Z_6(X,Z)k^2]k$$
$$\langle X,k \mid H \mid Z,k\pm 1\rangle = (1/2)G_b(X,Z) \times [J(J+1) - k(k\pm 1)]^{1/2}$$
$$\langle X,k \mid H \mid Z,k\pm 2\rangle = \pm(1/2)Z_1(X,Z)\{[J(J+1) - k(k\pm 1)] \times [J(J+1) - (k\pm 1)(k\pm 2)]\}^{1/2}.$$

Here, W is the homogeneous (Fermi-type) parameter, G_a, G_b, and G_c are Coriolis parameters, and the Z are higher order parameters. When Fermi interactions were present, we fitted in terms of the *perturbed* band origins (the actual positions of the $J_{KaKc} = 0_{00}$ levels) since these are physically well-determined and the resulting fit is less highly correlated [27] than if the deperturbed band origins are used.

The analysis began by using the propynal ground state rotational parameters determined by Winnewisser [5]. However, small discrepancies were noted in ground state combination differences for higher values of K_a, for example a discrepancy of about 0.01 cm^{-1} for the interval $K''_a = 6$ to 8. This problem arises because it was not possible for Winnewisser to determine a value for the parameter H_K. We therefore re-fitted the data of [5] together with a limited set of our own combination differences to determine a new set of ground state parameters, as listed in the last column of Table 1. These are essentially equivalent to those in [5] except for our inclusion of H_K and use of the A-reduced Hamiltonian.

3.2. The ν_7 and ν_{11} fundamental bands

An overview of the propynal spectrum studied here is shown in Fig. 2. As noted by Tavladorakis and Parkin [16] in their medium-resolution study of the ν_7 and ν_{11} fundamentals of the isotopomer

Table 1
Vibrationally diagonal parameters for the coupled 11^1, 7^1, 9^3, and 8^1 states from a 4-state fit and for the ground state of propynal (in cm^{-1})[a]

	11^1	7^1	9^3	8^1	Ground state
T_0	692.7707(1)	651.3143(1)	618.1922(11)[b]	614.0146(1)[b]	0.0
A	2.28071(421)	2.24841(430)	1.889140(240)	2.303666(144)	2.2694121(13)
B	0.1609133(22)	0.1611490(13)	0.1632442(145)	0.1608494(27)	0.16098780(20)
C	0.15017801(73)	0.15012496(71)	0.1512492(166)	0.1498450(25)	0.15008782(20)
$10^3 \times \Delta_K$	0.3145(292)	0.2792(299)	−0.6127(139)	0.30742(83)	0.29996(29)
$10^5 \times \Delta_{JK}$	−0.6383(17)	−0.3417(22)	−0.266(30)	−0.50396(117)	−0.49382(13)
$10^7 \times \Delta_J$	0.63972(95)	0.63735(98)	0.6380	0.6335(17)	0.6380(13)
$10^5 \times \delta_K$	0.1159	0.1159	−0.165(67)	0.1159	0.1159(94)
$10^7 \times \delta_J$	0.11528	0.11528	0.11528	0.1196(24)	0.11528(39)
$10^7 \times H_K$	1.59(32)	−0.152(294)	−15.51(84)	0.8366(117)	0.786(20)
$10^9 \times H_{KJ}$	−0.2756	−0.2756	−0.2756	−0.360(111)	−0.2756(39)
$10^{10} \times H_{JK}$	−0.237	−0.237	−0.237	−0.237	−0.237(16)

[a] Quantities in parentheses correspond to 1σ from the least-squares fit. Parameters without an uncertainty were fixed at the indicated values. These parameters go together with those in Table 2.
[b] These are the *perturbed* vibrational origins (see text), that is, the actual energies of the $J_{KaKc} = 0_{00}$ levels. The deperturbed origins are: 617.5954 and 614.6113 cm^{-1}.

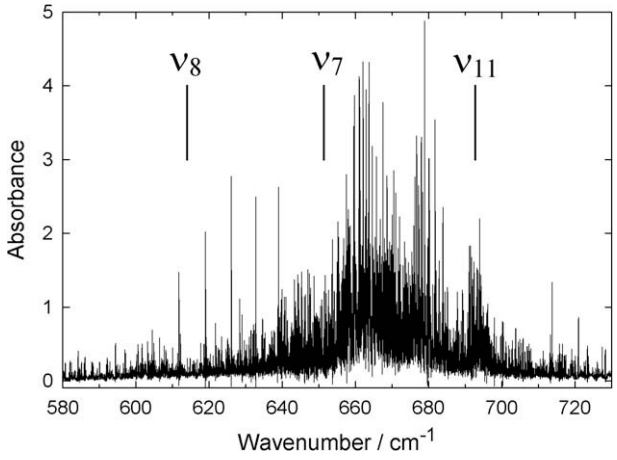

Fig. 2. An overview of the observed spectrum of propynal at 215 K. The origins of the three fundamental bands studied here, which are indicated, are not particularly obvious in the spectrum. The strongest absorption features are piled up in the crowded region between the ν_7 and ν_{11} band origins.

C_2HCDO, the large *a*-type Coriolis interaction between these vibrations has two dramatic effects. First, it greatly increases the effective *A* rotational constant of the 11^1 state and decreases that of the 7^1 state. Second, it causes a transfer of intensity from the *r*-type ($\Delta K_a = +1$) to *p*-type ($\Delta K_a = -1$) subbands of the ν_{11} band and conversely from the *p*-type to *r*-type subbands of ν_7. A combination of these effects results in the pile-up of intense absorption in the region between the ν_7 and ν_{11} band origins which is evident in Fig. 2.

Our analysis began in the less crowded and more weakly absorbing regions above the ν_{11} origin and below the ν_7 origin, with perpendicular subbands for higher K_a-values where asymmetry doubling was not resolved. As the assignments proceeded, we moved in towards the central region for the subbands involving $K'_a = 3, 2, 1$, and 0 for which asymmetry effects are significant. The process was reasonably straightforward, and from the beginning we included the ν_7/ν_{11} Coriolis interaction in a two-state fit. To illustrate the spectrum, Figs. 3 and 4 show a series of observed and simulated ${}^pQ_K(J)$ branches for ν_7 and ${}^rQ_K(J)$ branches for ν_{11}. Although some transitions in these *Q*-branches were included, the main foundation of the fit was provided by ${}^pP_K(J)$ lines for ν_7 and by ${}^rR_K(J)$ lines for ν_{11}, which are widely-spaced and tend to be unblended and easy to assign. In contrast, the *r*-type subbands of ν_7 and *p*-type subbands of ν_{11} tended to be impossibly congested, and the parallel *a*-type component ($\Delta K_a = 0$) of ν_7 was relatively weak (and also congested).

After assigning hundreds of transitions for each of the ν_7 and ν_{11} bands, we found that it was not possible to obtain a satisfactory fit, even with the two-state Hamiltonian including Coriolis and higher-order parameters. It was evident that there must be further relevant interactions involving additional vibrational states, and we thus turned our attention to the ν_8 band, expected [7] to be centered at 614 cm^{-1}.

3.3. The ν_8 fundamental band and the 8^1–9^3 interaction

In the region around 575–595 cm^{-1}, where we had already assigned some *p*-type subbands of ν_7 (Fig. 3), there were additional ${}^pQ_K(J)$ branches which could be assigned without too much difficulty to the ν_8 band. These are illustrated in Fig. 5 for $K'_a = 5$ to 8. The inclusion of these new data in a three-state analysis resulted in a notable improvement to the fit of the existing ν_7 and ν_{11} band transitions. But the quality of the fit was still much worse than the experimental accuracy. Moreover, it proved difficult to extend the assignment of the ν_8 band to lower values of K'_a. We managed to locate $K'_a = 4$, for which the ${}^pQ_5(J)$-branch is located near 596.55 cm^{-1} (not shown here), but these levels were seriously displaced (≈0.1 cm^{-1}) to higher wavenumber from the positions expected on the basis of the fit to $K'_a = 5$ to 8. Many checks, alternate assignments, and higher-order parameters were tried, but there was no way that a three-state analysis could account for our data. The fits of the ν_7 and ν_{11} bands were (by now) not so bad, but a meaningful fit to the ν_8 band seemed hopeless.

A long struggle to achieve a satisfactory analysis then took place, but we will not attempt to describe this struggle in detail. Clearly there were significant interactions involving one or more additional vibrational states, and it was not difficult to identify the most likely culprit, namely the 9^3 state (see Fig. 1). On the basis of previous data [7], we expected the origin of 9^3 to be 615.9 cm^{-1} (harmonic approximation), just 2.2 cm^{-1} above that of 8^1. Our eventual successful solution of the analysis struggle involves a four-state Hamiltonian (9^3, 8^1, 7^1, 11^1). It is difficult to be sure that this solution is unique in all details, but we believe that it is substantially correct. As outlined below (Section 4.3), the remaining discrepancies can probably be accounted for in terms of a fifth interacting state, $9^2 12^1$ (see Fig. 1), which, however, we did not include. A satisfying aspect of the four-state fit is that it enabled us to locate and assign the "missing" transitions of the ν_8 band involving the $K'_a = 0$, 1, 2, and 3 levels. Indeed, for $K'_a = 3$, we observed both the 8^1 ("bright") and 9^3 ("dark") upper states, which turn out to be almost completely mixed.

The 8^1 and 9^3 vibrational states both have A' symmetry, and the main effect linking them is a homogeneous Fermi-type interaction. But the consequences of this interaction are somewhat subtle and

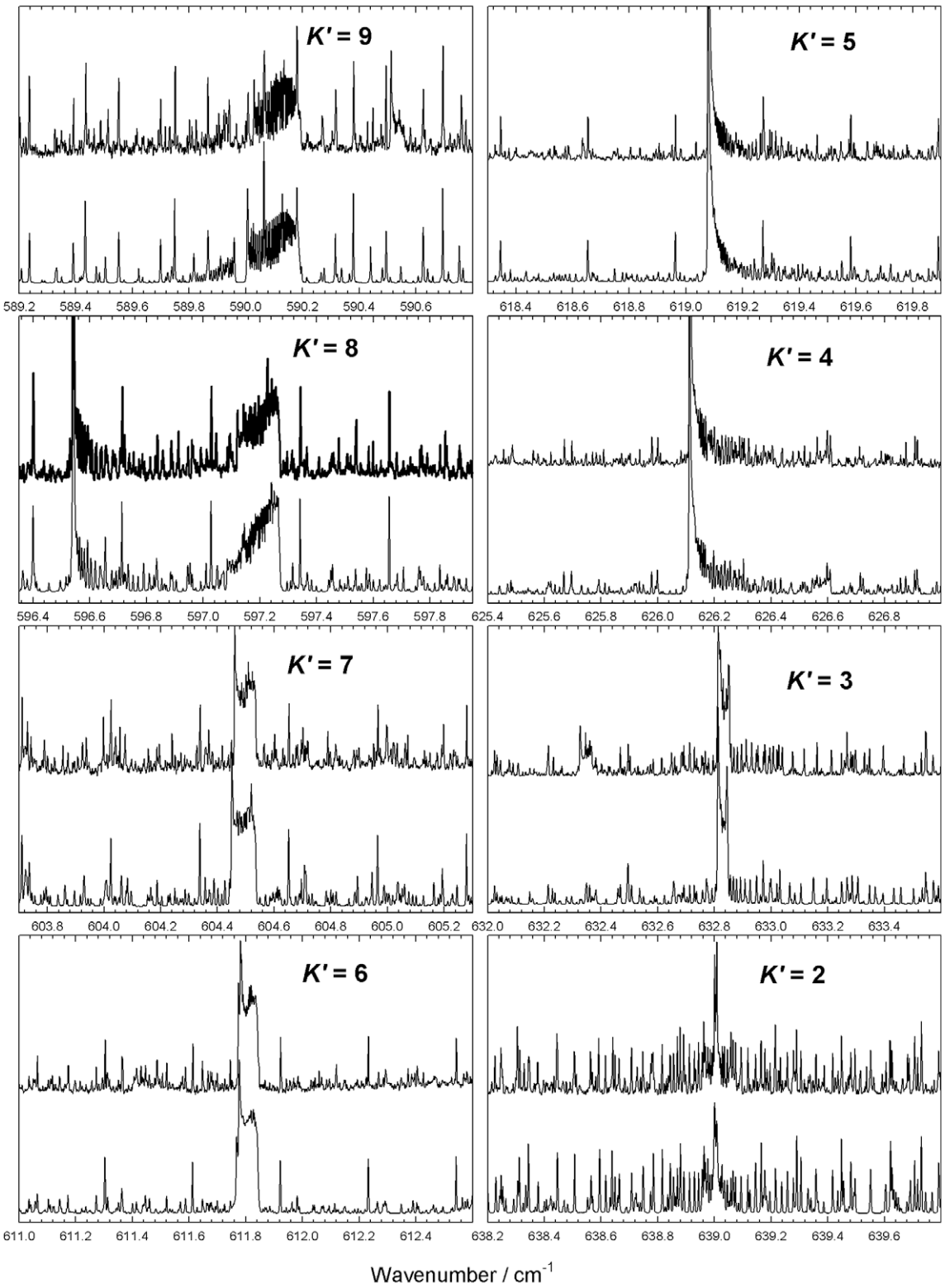

Fig. 3. Portions of the observed (upper traces) and simulated (lower traces) of propynal, showing ${}^{P}Q_K(J)$ branches of the ν_7 band. Note the gap in ${}^{P}Q_{10}(J)$ (i.e. $K'_a = 9$) which is due to a perturbation involving $K'_a = 10$ levels of the 9^3 vibrational state.

unexpected for the following reason: even though the origin of 9^3 is slightly above that of 8^1, its effective A rotational constant is considerably smaller. Thus the $K'_a = 0$, 1, and 2 levels of 9^3 lie above those of 8^1 (so the Fermi interaction "pushes" these 8^1 levels down), but the $K'_a = 4$, 5, 6, etc., levels of 9^3 lie below those of 8^1 (so the Fermi interaction pushes these 8^1 levels up). The $K'_a = 3$ levels of the two states are almost coincident in zeroth order, and so become highly mixed by the Fermi interaction. The situation is illustrated in Fig. 6, which is a calculated energy level diagram showing $J = 12$ levels of the 8^1 and 9^3 vibrational states. The deperturbed (zeroth order) levels are on the outside, and the actual (perturbed) levels on the inside, as indicated at the top of the figure. Perturbations of higher ($K'_a > 5$)

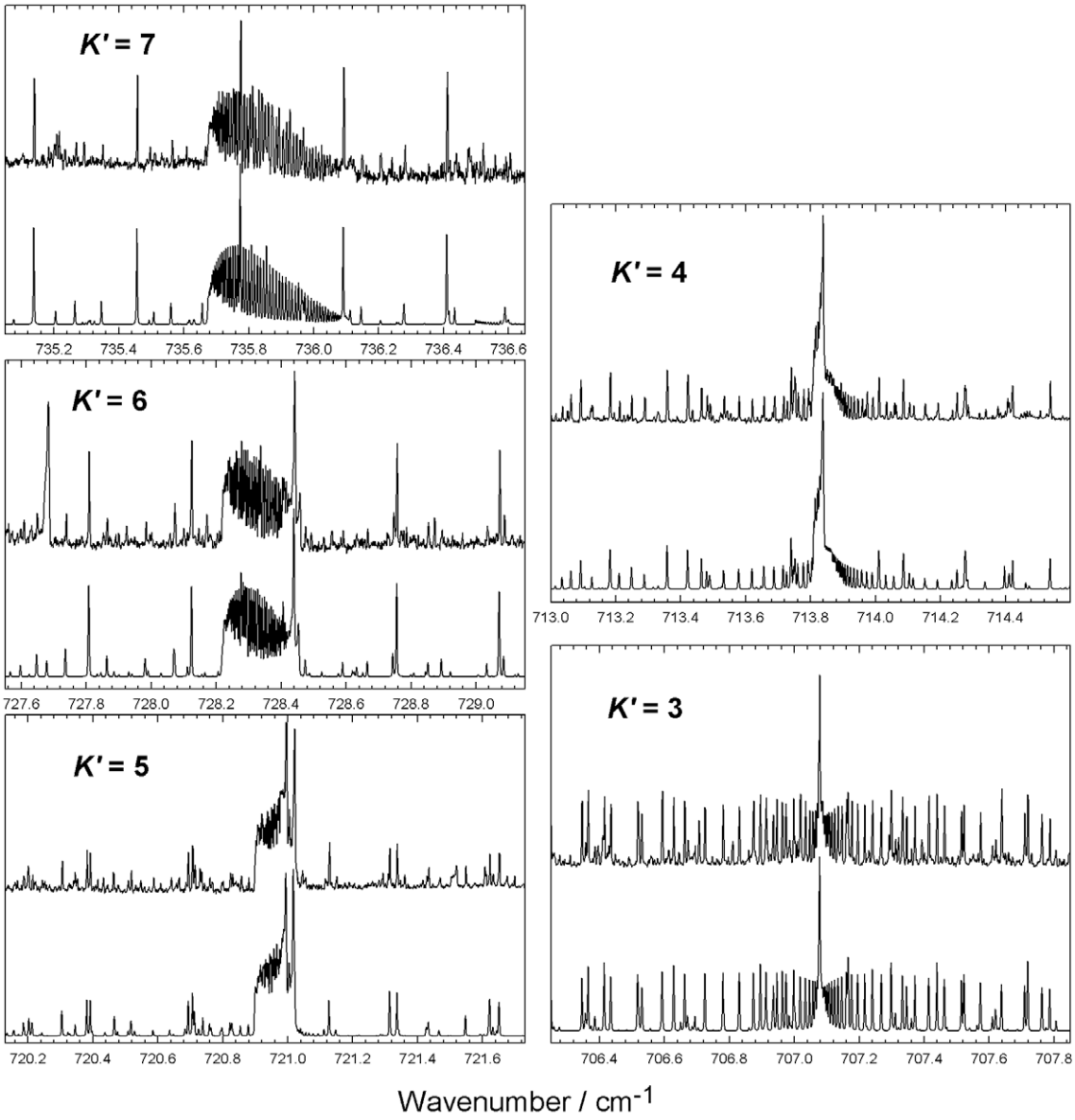

Fig. 4. Portions of the observed (upper traces) and simulated (lower traces) of propynal, showing ${}^{r}Q_K(J)$ branches of the ν_{11} band.

levels become progressively smaller since 8^1 and 9^3 become increasingly out of step with each other, which explains why the $K'_a = 4$ levels of 8^1 were observed to be pushed up relative to our original expectations. The K'_a = 0–3 levels are massively affected, which explains why we originally could not find them at all.

3.4. The four-state fit

Our final fit included a total of about 1400 transitions, of which about 670 were from the ν_7 band, 420 from the ν_{11} band, and 310 from the ν_8 band (including a few perturbation-allowed transitions of $3\nu_9$). These are listed in Tables A1, A2, and A3 of the Appendix. The data include many transitions with values of J' up to about 40, and, in a few cases, 49. The range of K'_a-values is from 0 to 11 for the ν_7 band, from 0 to 7 for ν_{11}, and from 0 to 9 for ν_8. Transitions which were blended, very weak, or very strong (saturated) were given weights of 0.1 or zero in the fit. The choice of which parameters to vary was difficult, and necessarily somewhat arbitrary. In the end we settled on a set of 47 parameters, with results as listed in Tables 1 and 2. The quality of the fit was quite good, with root mean square deviations of only about 0.0003 cm^{-1} for 1179 transitions with unity weight, 0.0008 cm^{-1} for 134 transitions with weight of 0.1, and 0.010 cm^{-1} for 92 transitions with zero weight. Many of the zero weight transitions occur in regions of local perturbations, as discussed below in Section 4.3.

With the help of the PGopher program [23], we attempted to get an approximate idea of the relative values of the various transition dipole moments involved in the spectrum. Starting with an arbitrary *c*-type transition moment of 1.0 for the ν_{11} band, satisfactory agreement with the observed spectrum was obtained with the following relative dipole moments: 1.0 for the ν_7 *b*-axis component, 0.25 for the ν_7 *a*-axis component, −0.25 for the ν_8 *b*-axis component, 0.15 for the ν_8 *a*-axis component, and zero for the $3\nu_9$ band moments.

4. Discussion and conclusions

4.1. General discussion of parameters

The band origin determined in 1963 by Brand et al. [7] for ν_{11}, 692.7 cm^{-1}, is in almost perfect agreement with our value of

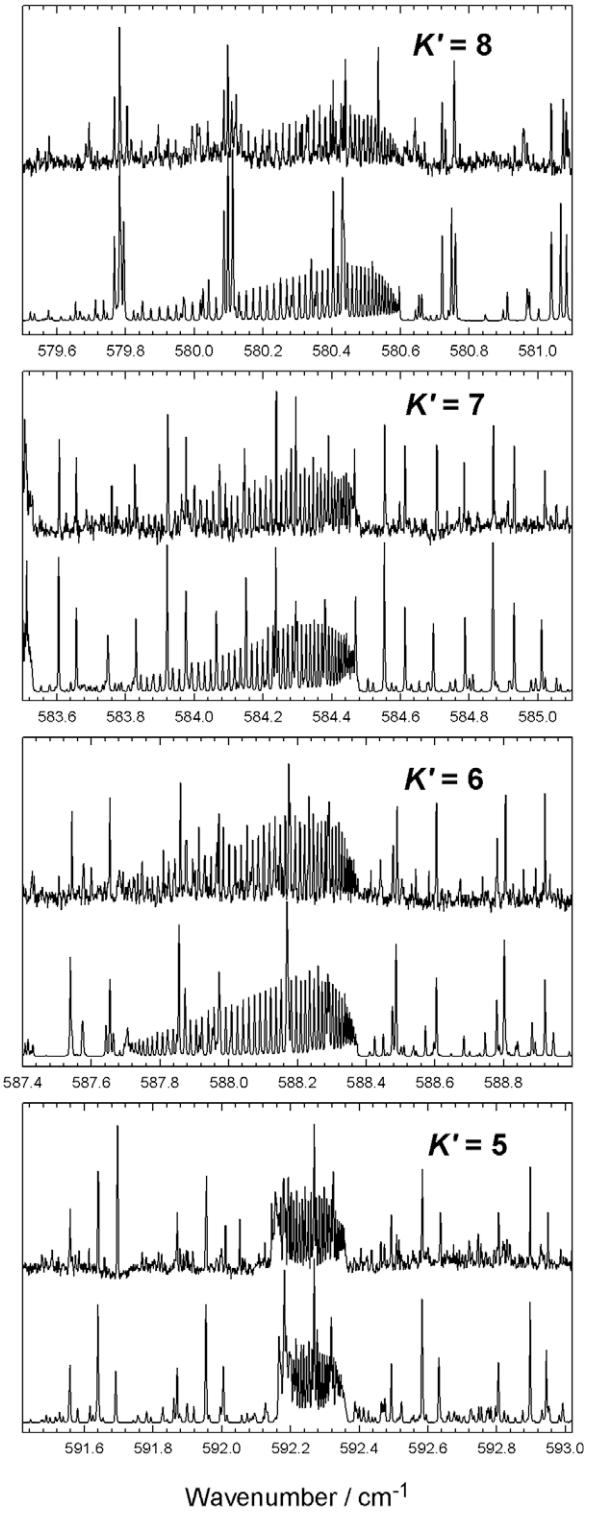

Fig. 5. Portions of the observed (upper traces) and simulated (lower traces) of propynal, showing ${}^{P}Q_K(J)$ branches of the ν_8 band.

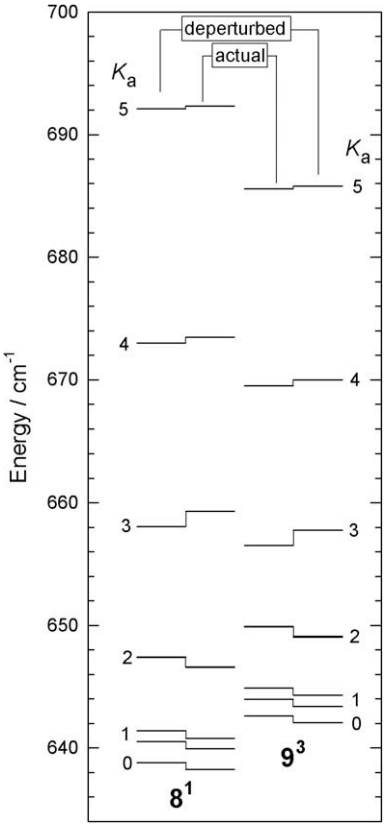

Fig. 6. Calculated energy levels of propynal for the 8^1 and 9^3 vibrational states with $J = 12$. The origin of 9^3 lies above that of 8^1, but the A rotational constant of the former is smaller, and so the deperturbed (zeroth-order) levels for $K_a = 3$ are almost coincident. When the Fermi-type interaction is "turned on", levels of 8^1 with $K_a < 3$ are "pushed down" while those with $K_a > 3$ are "pushed up".

Table 2
Vibrationally off-diagonal parameters for the coupled 11^1, 7^1, 9^3, and 8^1 states of propynal from a 4-state fit (in cm^{-1})[a]

	X, Y	
	$7^1, 8^1$	$8^1, 9^3$
$W(X, Y)$	0.0	1.46180(81)
$Z_2(X, Y)$	0.0	−0.009139(100)
$G_c(X, Y)$	0.0	0.008038(32)
$10^3 \times Z_1$(X,Y)	−0.1294(21)	0.0319(58)
$10^4 \times Z_3$(X,Y)	0.0	0.805(58)
	X, Z	
	$7^1, 11^1$	$11^1, 8^1$
$G_a(X, Z)$	4.2599(209)	0.8326(67)
$G_b(X, Z)$	0.07729(34)	−0.07713(55)
$10^3 \times Z_6(X, Z)$	−1.25(13)	0.00416(21)
$10^4 \times Z_1(X, Z)$	0.249(65)	0.0

[a] Quantities in parentheses correspond to 1σ from the least-squares fit. These parameters go together with those in Table 1.

692.7707 cm^{-1}, while their value for ν_7 was low by 1.3 cm^{-1} (650.0 vs. 651.3413 cm^{-1}), and that for ν_8 was low by 0.3 cm^{-1} (613.7 vs. 614.0146 cm^{-1}). The large a-type Coriolis interaction between the 7^1 and 11^1 vibrational states is characterized by the parameter $G_a(7^1, 11^1) = 4.26\ cm^{-1}$, which implies a value of about $\zeta^{(a)}_{7,11} = 0.939$ for the dimensionless Coriolis zeta, slightly larger than previous determinations of 0.922 [7] or 0.92 (for C_2HCDO) [16]. If one tries to fit the spectrum (or energy levels) without including this interaction, then one obtains quite disparate values for the a-axis parameters: for example, effective A- and Δ_K-values of about 1.84 and −0.0024 cm^{-1} for the 7^1 state and about 2.70 and +0.0028 cm^{-1} for 11^1. But with the Coriolis interaction properly accounted for, these parameters retain their normal values, as seen in Table 1 where the A-values for 7^1, 11^1, and the ground state are all within 0.033 cm^{-1} of one another. The B and C rotational constants in these two excited states also change very little (<0.1%) from the ground state values.

Interestingly, we also determined a smaller but still substantial *a*-type Coriolis interaction connecting the 8^1 and 11^1 states, $G_a(8^1, 11^1) = 0.83\ \mathrm{cm}^{-1}$. Since 7^1 and 11^1 are already highly mixed, this automatically gives an effective mixing of 8^1 and 7^1, which becomes stronger as K_a increases, and which is important since 7^1 is located closer to 8^1 than is 11^1. But the most significant perturbation of the 8^1 state is due to 9^3, as already mentioned. Our analysis indicates that the unperturbed origin of 9^3 lies just $2.98\ \mathrm{cm}^{-1}$ above that of 8^1, a separation which increases to $4.18\ \mathrm{cm}^{-1}$ when the Fermi interaction is "turned on". This interaction was illustrated in Fig. 6 and is further explored below in Section 4.2. Its consequences are particularly prominent because the values of the rotational constants, A and $(B + C)/2$, are rather different for the two states, which results in many level crossings.

Since only a few transitions actually involving the 9^3 state were observed, one might question whether the values obtained here for its rotational constants (Table 1) are meaningful. It seems reasonable that the effective A value in 9^3 should be low, as observed, since we expect a substantial *a*-type Coriolis interaction between the ν_9 and ν_{12} modes. More quantitatively, we can estimate the effects of this interaction on the 9^3 state by setting up a four-state calculation involving the 9^3, $9^2 12^1$, $9^1 12^2$, and 12^3 states (see Fig. 1). We assume that each state starts with ground state rotational parameters, and that their successive separations are $61.2\ \mathrm{cm}^{-1}$, as given by the harmonic approximation and the fundamental frequencies from [7]. In the calculation, the actual interactions between 9^3 and $9^2 12^1$, and between $9^1 12^2$, and 12^3, are expected to be $\sqrt{3} \times G_a(9, 12)$, and that between $9^2 12^1$ and $9^1 12^2$ is expected to be $2 \times G_a(9, 12)$, where $G_a(9, 12)$ denotes the *a*-type Coriolis interaction between the fundamental states 9^1 and 12^1. It then turns out that a value of about $G_a(9, 12) = 2.65\ \mathrm{cm}^{-1}$ is needed in order to give an effective value of $A = 1.89\ \mathrm{cm}^{-1}$ as observed for 9^3. This implies that $\zeta^{(a)}_{9,12} = 0.58$, which is a bit smaller than the value of 0.639 obtained from the electronic spectrum [7]. In other words, the effective A-value for the 9^3 state should be at least as small as we obtained, if not slightly smaller. Turning to the B and C values, we know from early microwave work on propynal [3] that the value of $(B + C)/2$ for the 9^1 state is about 0.26% higher than in the ground state, and on this basis our value for 9^3, which is about 1.1% higher than the ground state, seems acceptable. Moreover, in 1980 Jones [14] reported an approximate determination of B and C for the 9^3 state, based on unpublished microwave data. These values (0.1628 and $0.1511\ \mathrm{cm}^{-1}$) are quite close to ours (0.1632 and $0.1512\ \mathrm{cm}^{-1}$), especially considering the fact that his analysis may have been contaminated by effects of the interaction with the 8^1 state. In conclusion, we believe that the 9^3 state parameters in Table 1 are realistic, although direct observation of a wider range of transitions involving this state would of course be desirable.

Returning to the well-characterized states 11^1, 7^1, and 8^1, we can also compare our B and C values with those of Jones [14], bearing in mind that we do not expect perfect agreement since our analysis incorporates various Coriolis and Fermi interactions while his single-state analysis gives effective parameters. The agreement is actually rather good (better than $0.00014\ \mathrm{cm}^{-1}$ or 0.09%), as long as we interchange Jones' labels for ν_7 and ν_8, which were only tentative since they were based on small differences in observed microwave intensities.

4.2. General discussion of perturbations

There are many perturbations in the propynal spectrum analyzed here. Some of these are global in nature, affecting many rotational levels, like those caused by the large *a*-type Coriolis interaction between the 11^1 and 7^1 states which become especially significant as K_a increases. Other perturbations are local in nature, affecting a limited number of levels, particularly where a series of levels of one vibrational state crosses a series from another state. The various perturbations can be examined in detail using the listing of calculated energy levels given in Table A4 of the Appendix, which is based on the molecular parameters from Tables 1 and 2. However, the limits of validity of this table should be kept in mind; for example, our observations of the ν_{11} band extend only up to $K_a = 7$, so the calculations beyond this point represent an extrapolation. In particular, the calculated levels for the 9^3 state are obviously less certain than the others since only a few transitions directly involving this state were observed.

Perhaps the most dramatic perturbation encountered here is that affecting the $K_a = 3$ levels of the 8^1 and 9^3 states, which are almost coincident in the zeroth order calculation before the Fermi interaction is turned on, as shown in Fig. 6. The mixing of $K_a = 3$ is sufficiently large that we were able to observe transitions to both the bright 8^1 levels and the dark 9^3 levels. Thus there are two observed ${}^pQ_4(J)$ branches (the first around $598.5\ \mathrm{cm}^{-1}$ and the second, somewhat weaker, around $601.3\ \mathrm{cm}^{-1}$), together with accompanying ${}^pP_4(J)$ branches. Since the first of these ${}^pQ_4(J)$ branches is stronger, it seems evident that the "true" $K_a = 3$ levels of the 8^1 state lie below those of the 9^3 state. However, our computer program actually labels these levels the other way around for $J < 18$, and we retain this automated labeling in Fig. 6 and Table A4. The explanation of this paradox is straightforward, but a bit subtle. The computer labeling is based on calculated eigenvectors: although the program tries to make intelligent choices, the "winner" tends to be whichever basis state makes the largest contribution to each level. But the 8^1 state is already fragmented by interactions with 11^1 and 7^1, so it tends to be "weakened" in the "competition" with 9^3. The observed transitions involving the $K_a = 3$ levels of 9^3 are included along with the main 8^1 transitions in Table A3 of the Appendix (but recall that the vibrational labeling is a bit arbitrary). The $K_a = 4$ and (especially) 2 levels of 8^1 and 9^3 are also rather mixed, but for these we were only able to assign transitions to the dominant 8^1 levels. Transitions to the dark 9^3 levels were too weak to detect reliably, even though we had a pretty good idea of their expected locations.

4.3. Local perturbations of the 7^1 state

We observed a series of local perturbations affecting $K'_a = 9$, 10, 11, and 12 levels of the 7^1 state. For $K'_a = 9$, the crossing is visible as a gap in the ${}^pQ_K$ – branch (see Fig. 3) but it occurs at a J-value higher than our assignments extended. For $K'_a = 10$, there are two level-crossings, the first at $J = 22$ and another at $J = 33$. For $K'_a = 11$, there is one crossing at $J = 24$, and for $K'_a = 12$, there is one at $J = 27$. These perturbations are quite visible in the relevant ${}^pQ_K(J)$ branches, as illustrated in Fig. 7 for $K'_a > 9$. They could also be assigned in the ${}^pP_K(J)$ branches for $K'_a = 10$ and part of 11, but not for $K'_a = 12$ because of the cutoff of our experimental spectrum at $570\ \mathrm{cm}^{-1}$. As our analysis proceeded, it became evident that some of these perturbations were almost certainly caused by $\Delta K_a = 1$ interactions with the 9^3 state (e.g. $K_a = 11$ of 9^3 perturbing $K_a = 10$ of 7^1). But not all of them, since there was no way to explain two crossings of the $K'_a = 10$ stack. Deciding on the most likely assignment was tricky, but we eventually chose a solution in which the 9^3 state was responsible for the $K'_a = 10$ crossing at $J = 34$, and for all the $K'_a = 9$, 11, and 12 crossings. We explicitly included in the final least-squares fit the 7^1 transitions for $K'_a = 11$, both below and above the crossing point. Interestingly, this perturbation could be fit very well without introducing any new parameters. Even with no direct interaction linking 7^1 with 9^3, the existing indirect link (proceeding mostly from 9^3 through 8^1 through 11^1 to 7^1) was just right!

The $K'_a = 12$ levels of 9^3 responsible for perturbing $K'_a = 11$ of 7^1 were now effectively pinned down in the fit. This then resulted in a

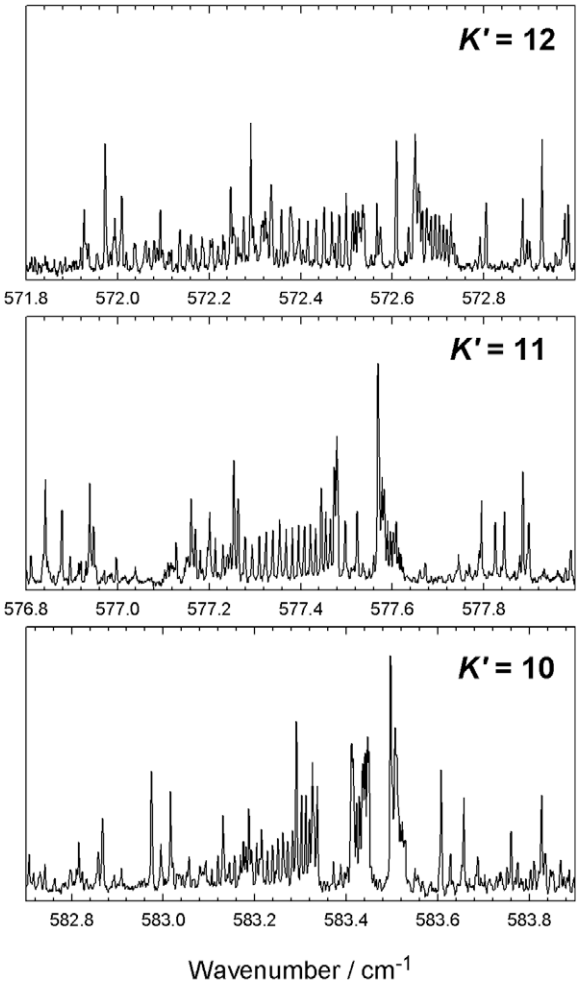

Fig. 7. Observed ${}^{P}Q_K(J)$ branches of the ν_8 band of propynal with $K'_a = 10, 11$, and 12, showing gaps due to level-crossing perturbations. Note that there are two gaps for $K'_a = 10$.

predicted crossing of the $K'_a = 9$ stack of 7^1 by $K'_a = 10$ of 9^3 between $J = 45$ and 46, in qualitative agreement with the spectrum (Fig. 3). It predicted a crossing of the $K'_a = 10$ stack of 7^1 by $K'_a = 11$ of 9^3 between $J = 32$ and 33, close to what was observed in the spectrum. The quality of the fit here was thus improved, but it was still not great. We blame the remaining disagreement on the effect of the other (as yet unexplained) crossing of the $K'_a = 10$ stack at $J = 22$, and decided to give zero weight to all transitions involving 7^1 state levels with $K'_a = 10$ and $J > 12$. For the 7^1 state levels with $K'_a = 12$, the analysis predicted a crossing by 9^3 levels with $K'_a = 13$ between $J = 29$ and 30, again close to what is observed in the spectrum. (Note that there was a labeling problem for the $K_a = 12$ levels – see Table A4). However, it was not possible to include any $K'_a = 12$ transitions of 7^1 in the analysis, mainly because the ${}^{P}P_{13}(J)$ branch was outside the range of our spectrum so that the exact numbering of the ${}^{P}Q_{13}(J)$ branch could not be confirmed.

What about the unexplained crossing of the $K'_a = 10$ stack of 7^1 at $J = 22$? It is very likely that this is due to an interaction with the $9^2 12^1$ state, which lies approximately 20 cm^{-1} higher than 7^1 (see Fig. 1). We estimate that the $K'_a = 9$ levels of $9^2 12^1$ should occur very close to $K'_a = 10$ of 7^1, based on the four-state calculation described above in Section 4.1. Moreover, it is clear that further perturbations of 7^1 by $9^2 12^1$ are probable for other K_a-values, and it is thus no wonder that we encountered some difficulties in fitting perfectly all these perturbations in the $K'_a = 9$ to 12 range without the inclusion of the $9^2 12^1$ state. We considered trying an analysis with five (or more) interacting vibrational states, but decided against it for a number of reasons. Most importantly, it was possible to achieve an excellent fit to most of the observed spectrum for $J < 40$ with the four-state analysis reported here. If more states were added, there would be relatively little unexplained experimental data to help constrain their parameters. And if the $9^2 12^1$ state were included, then it would be difficult not to include the $9^1 12^2$ and 12^3 states as well! Furthermore, there are serious practical problems, not so much in the computing power or time required, but rather in the challenge of sorting and labeling the energy levels, which rapidly becomes more difficult as more states are included in a fit.

4.4. Conclusions

The ν_7, ν_8, and ν_{11} fundamental bands of propynal, C_2HCHO, in the 600–700 cm^{-1} range have been observed with high spectral resolution (~0.003 cm^{-1}) and rotationally analyzed in detail. Coriolis interactions among the three upper states, 7^1, 8^1, and 11^1 are significant and were included in the analysis. A satisfactory fit to the observations could not be achieved without the inclusion of a fourth vibrational state, 9^3, because there is a significant Fermi-type interaction between 9^3 and 8^1 which has important effects on the spectrum. The resulting four-state analysis, which is reported here, accounts very well for most of the observed spectrum for J-values up to 40 or 50. We believe that this work represents the first systematic high-resolution infrared study of propynal. In the future, it would be worthwhile to extend this work into the far infrared region in order to study the lowest-lying fundamentals, ν_9 and ν_{12} in the 200–300 cm^{-1} range, and their binary combinations, the 9^2, $9^1 12^1$, and 12^2 states in the 500 cm^{-1} range. As well, it should now be relatively straightforward to extend the analysis of the pure rotational spectra of excited vibrational states of propynal by means of microwave, millimeter wave, and far-infrared FT spectroscopy.

Acknowledgments

We wish to thank Stephane Denommée and Bill Neil for their assistance with the synthesis of propynal and the acquisition of the spectrum, and the National Science Council of Taiwan (Grant No. NSC93-2113-M-009-018) for support.

Appendix A. Supplementary data

Supplementary data for this article (Tables A1–A4) are available on ScienceDirect (www.sciencedirect.com) and as part of the Ohio State University Molecular Spectroscopy Archives (http://library.osu.edu/sites/msa/jmsa_hp.htm). Supplementary data associated with this article can be found, in the online version, at doi:10.1016/j.jms.2008.09.002.

References

[1] W.M. Irvine, R.D. Brown, D.M. Cragg, P. Friberg, P.D. Godfrey, N. Kaifu, H.E. Matthews, M. Ohishi, H. Suzuki, H. Takeo, Astrophys. J. 335 (1988) L89–L93.
[2] S. Petrie, Astrophys. J. 454 (1995) L165–L168.
[3] J.A. Howe, J. H Goldstein, J. Chem. Phys. 23 (1955) 1223–1225.
[4] C.C. Costain, J.R. Morton, J. Chem. Phys. 31 (1959) 389–393.
[5] G. Winnewisser, J. Mol. Spectrosc. 46 (1973) 16–24.
[6] J.C.D. Brand, J.H. Callomon, J.K.G. Watson, Can. J. Phys. 39 (1961) 1508–1510.
[7] J.C.D. Brand, J.H. Callomon, J.K.G. Watson, Disc. Faraday Soc. 35 (1963) 175–183.
[8] J.C.D. Brand, J.K.G. Watson, Trans. Faraday Soc. 56 (1960) 1582–1590.
[9] G.W. King, D. Moule, Spectrochim. Acta 17 (1961) 286–290.
[10] C.A. Rogaski, A. Wodkte, J. Chem. Phys. 100 (1994) 78–87.
[11] M. Takami, K. Shimoda, J. Mol. Spectrosc. 59 (1976) 35–42.
[12] M. Takami, M. Suzuki, J. Mol. Spectrosc. 73 (1978) 144–153.

[13] M. Takami, M. Suzuki, J. Chem. Phys. 72 (1980) 4089–4098.
[14] H. Jones, J. Mol. Spectrosc. 81 (1980) 21–36.
[15] Th. Walter, H. Bitto, T.K. Minton, J.R. Huber, Chem. Phys. Lett. 231 (1994) 64–69.
[16] K. Tavladorakis, J.E. Parkin, Spectrochim. Acta A 52 (1996) 1823–1827.
[17] K. Tavladorakis, J.E. Parkin, Spectrochim. Acta A 52 (1996) 629–635.
[18] H. McNab, G. Morel, E. Stevenson, J. Chem. Res. (S) (1997) 37.
[19] J.W.C. Johns, Mikrochim. Acta (Wien) III (1987) 171–188.
[20] J.W.C. Johns, Z. Lu, A.R.W. McKellar, J. Mol. Spectrosc. 159 (1993) 210–216.
[21] A.R.W. McKellar, Faraday Discuss. Chem. Soc. 97 (1994) 69–80.
[22] Available from: <http://physics.nist.gov/Divisions/Div844/facilities/uvs/jb95userguide.htm>.
[23] PGOPHER, a Program for Simulating Rotational Structure, C.M. Western, University of Bristol, U.K., Available from: <http://pgopher.chm.bris.ac.uk>.
[24] J.K.G. Watson, in: J.R. Durig (Ed.), Vibrational Spectra and Structure 6 (1977) 1–89.
[25] Y. Xu, J.W.C. Johns, A.R.W. McKellar, J. Mol. Spectrosc. 168 (1994) 147–157.
[26] A.R.W. McKellar, D. Tokaryk, L.-H. Xu, D.R.T. Appadoo, T. May, J. Mol. Spectrosc. 241 (2007) 31–38.
[27] A.R.W. McKellar, J.B. Burkholder, A. Sinha, C.J. Howard, J. Mol. Spectrosc. 125 (1987) 288–308.